Soft Matter

PAPER

View Article Online
View Journal | View Issue

Cite this: *Soft Matter*, 2026, **22**, 1679

Epoxy coating to prolong actuation time in degas-driven PDMS micropumps

Yara Alvarez-Braña,†[ab] Andreu Benavent-Claró, †[cd] Fernando Benito-Lopez,[b] Aurora Hernandez-Machado *[cd] and Lourdes Basabe-Desmonts*[ae]

Received 23rd September 2025,
Accepted 24th January 2026

DOI: 10.1039/d5sm00964b

rsc.li/soft-matter-journal

To enhance the portability of Lab-on-a-Chip technology, avoiding bulky electronic flow control systems is crucial. Self-powered microfluidics can significantly improve portability by eliminating the need for electronic components. Traditionally, self-powered microsystems handle small fluid volumes for up to one or two hours. However, many experiments, such as cell culture or real-time biomarker detection assays, require flow control for longer periods. In this study, we demonstrate that polymeric micropumps can provide self-powered flow control for intermediate durations, ranging from several to more than 10 hours. By monitoring the fluid front dynamics of a solution flowing through a microchannel over 1.5 meters long, we developed calibration curves for various micropump types. Our findings reveal that the pump's actuation time is influenced by degassing time, and effective surface area. Using these calibration curves, we compare mathematical models to predict flow rates and actuation times, facilitating the design of customized self-powered microsystems for both short and long-term applications. Epoxy-coated PDMS pumps represent a notable example of a long-operating self-powered microsystem, which holds significant potential for applications requiring controlled flow over extended periods.

1 Introduction

During the past decades, microfluidic technology has become an excellent tool for the development and manufacture of devices with applications in fields like biomedical diagnostics or cell biology research.[1,2] The development of self-powered platforms is an area on the rise, as these autonomous devices can generate flow inside the microfluidic channels without any source of external power, facilitating the transport and the use of these analytical platforms at the point of need.[3]

While early self-powered devices focused on short-term fluid control using finger-actuated pumps, paper-based systems, or effervescent micropumps,[4–6] many applications, such as continuous cell culture and microfluidics for real time monitoring, require precise, long-term flow control.[7–13] Despite advances, achieving long-term autonomous operation remains a significant challenge in microsystems.[14]

In 2004, Hosokawa *et al.*[15] reported a power-free pumping methodology based on the use of degas-driven flow in devices made of polydimethylsiloxane (PDMS) polymer. After degassing in a vacuum chamber, degas-driven flow utilizes the material's gas solubility to create a pressure gradient that drives liquid through a microchannel without external power enabling the movement of the sample through the channel, when placed at atmospheric conditions. Since then, degas-driven PDMS devices have been used in the microfluidic field,[16,17] leading to new strategies, such as the use of PDMS modular micropumps.[18] In this context, our group recently demonstrated that combining plastic cartridges with polymeric micropumps creates a universal modular architecture for self-powered microfluidics, capable of performing a wide range of fluidic operations and processing large volume samples. These systems have demonstrated the capability to handle a wide range of fluid volumes, offering high flow rates and prolonged autonomous operation, such as the 90 min of continuous flow achieved with PDMS micropumps. Additionally, the combination of modular micropumps made of different polymeric materials, with customizable 3D-printed microfluidic cartridges has proven to be a highly adaptable and efficient method for creating self-powered devices suitable for point-of-care applications, including blood analysis and colorimetric tests for starch detection.[19,20] However, extending operational durations beyond 90 min remains a crucial goal, but in this paper we demonstrate that we can go further using epoxy-coated PDMS pumps.[21]

[a] *Microfluidics Cluster UPV/EHU, BIOMICs Microfluidics Group, University of the Basque Country UPV/EHU, Vitoria-Gasteiz, Spain. E-mail: lourdes.basabe@ehu.eus*
[b] *Microfluidics Cluster UPV/EHU, Analytical Microsystems & Materials for Lab-on-a-Chip (AMMa-LOAC) Group, University of the Basque Country UPV/EHU, Vitoria-Gasteiz, Spain*
[c] *Condensed Matter Physics Department, Physics Faculty, University of Barcelona, Barcelona, Spain*
[d] *Institute of Nanoscience and Nanotecnology (IN2UB), University of Barcelona, Barcelona, Spain*
[e] *Basque Foundation of Science, IKERBASQUE, Vitoria-Gasteiz, Spain*
† Both authors are first authors.

With the aim of contributing to the development of self-powered microsystems capable of processing samples for prolonged durations, in this work, we evaluate the long-term performance of PDMS micropumps. To do that, we used "fluid front dynamics" which has been reported before as a tool to study capillary or pressure-driven filling of microchannels to characterize fluid properties.[22,23] In this work, we used fluid front dynamics to characterize PDMS pumps by observing and analyzing the movement of the liquid front within a microfluidic device. We monitored the front dynamics of a degas-driven fluid in an extended microchannel over 1.5 m long. By characterizing various pump parameters, such as degassing time, surface area, and recovery rate, we sought to determine if PDMS micropumps could sustain fluidic operations for periods longer than an hour. We compare our PDMS pumps experimental results with the mathematical model presented in reference.[24] Our study addresses a critical unmet need in the field and will contribute to the design of reliable, self-powered microsystems capable of processing samples for prolonged durations.

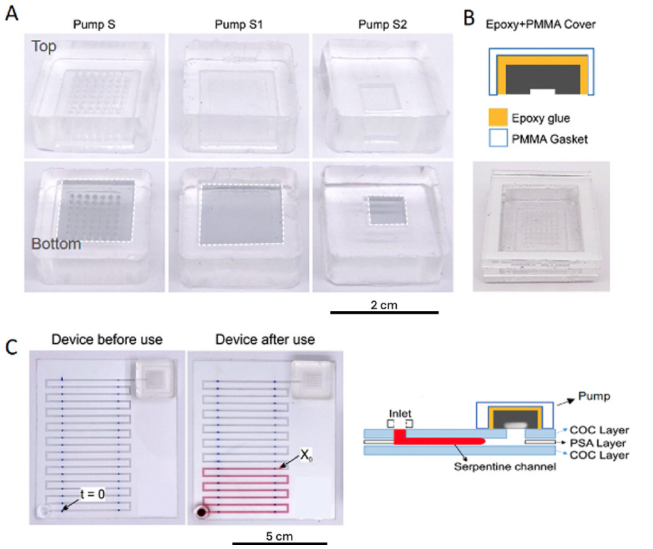

Fig. 1 Characterization of PDMS micropumps. (A) Two images of each of the three PDMS pumps used in the study are presented, distinguished by their effective surface area (Se). The top row shows the pumps placed upside down, while the bottom row shows the same pumps placed right side up to facilitate visualization of the effective surface area. The pumps are labeled as S, S1, and S2, with effective surface area (Se) values of 683 mm^2, 290 mm^2, and 92 mm^2, respectively. (B) Schematic drawing (top) and photograph (bottom) of an epoxy-coated micropump for long-term PDMS micropumps. (C) Photographs (left) and schematic side cut (right) of long serpentine cartridges used to monitor the fluid front dynamics driven by the PDMS micropumps.

2 Materials and methods

2.1 PDMS micropumps fabrication and actuation

Different PDMS micropumps were fabricated with SYLGARD 184 silicone elastomer kit by casting PDMS on a 3D printed mold using a previously described protocol.[19] Briefly, the curing agent and polymer base were mixed in ratios of 1 : 10, then degassed in a vacuum desiccator for 30 min to remove air bubbles. The degassed mixture was poured onto the negative mold (Fig. S1A), fabricated by stereolithography 3D printing. The polymer-mold ensemble was heated at 70 °C for 2 h to fully cross-link the PDMS. Finally, the cured PDMS part was peeled off from the mold, resulting in the micropumps (Fig. S1B). For each pump a different mold was used to obtain different effective surface areas (S = 683 mm^2, S1 = 290 mm^2 or S2 = 92 mm^2), (Fig. 1A). In particular, pump S was fabricated using a mold containing a 7 × 7 array of conical posts, which generated the complementary array of conical cavities in the PDMS matrix (previously described in ref. 19). This microstructured surface substantially increased the effective surface area of pump S compared to pumps S1 and S2. Two different sets of micropumps were fabricated, one set consisted of bare PDMS, non-coated PDMS pumps, and the other set of micropumps were epoxy coated micropumps, EPX-S, EPX-S1, EPX-S2. The second set was made to restrict the recovery of air through the external surfaces, allowing only the absorption of air through the effective surface area, in contact with the channel (Fig. 1A and B).

To create the epoxy coated micropumps, the bare PDMS pumps were covered with a layer of liquid epoxy adhesive (Epoxy Araldite, Ceys) and placed in an *ad hoc* premade PMMA gasket adjusted to the pumps size (Fig. 1B) to prevent the exchange of air through the external surfaces. The coating was applied to ensure a uniform 1 mm thickness of epoxy resin, well beyond the ≈ 100 μm threshold needed to minimize gas permeability. This gasket-based method produced a continuous, defect-free layer that adhered robustly to PDMS without delamination during operation. Therefore, the six manufactured pumps had different effective surface area (S_e), total surface (S_t) area and/or volume (Table S1). In epoxy-coated pumps, gas exchange occurs only through the effective surface area, while in non-coated pumps along the total surface. For this reason, under identical degassing conditions, coated pumps will be more efficient as they will only reabsorb air through the microfluidic channel where the sample liquid is located.

Manufactured micropumps were degassed in a RVR003H-01 vacuum chamber (Dekker Vacuum Technologies, USA) at a pressure of 70 Pa during different degassing times (ranging from 5 to 180 min) and vacuum packed in a SV-204 vacuum sealer (Sammic, Spain) to be stored in an airless environment until use. Device-to-device variability was assessed through replicate measurements (n = 3) for each pump condition. The observed variability in key parameters like X_0, consistent with prior studies on degas-driven systems, ranged from 5% to 12%. The values reported in this manuscript correspond to the average of these measurements.

2.2 Fabrication of the multilayer-plastic devices for front fluidics characterization

Polymeric microfluidic cartridges were fabricated by multiple-layer lamination. Microfluidic channels were cut using a Graphtec cutting Plotter CE6000-40 (CPS Cutter Printer Systems, Spain) on sheets of pressure sensitive adhesive (PSA) layers

(127-μm thick ARcare 8939 white PSA, Adhesive Research, Ireland) and a 140 μm thick COC substrate (mcs foil 011, Topas, microfluidic ChipShop, Germany) was used as the bottom base and top layer of the device. All the cartridges included a 4 mm diameter inlet and a 10 × 5 mm^2 ($W \times L$) outlet at the end of the channel used as waste reservoir. The assembly and lamination of the COC and PSA layers, one on top of the other, generated a microfluidic serpentine channel with a height of 0.127 mm, a width of 1 mm and a total length of 900 mm for the normal device; however, a longer channel 1800-mm long was used for the experiments with the epoxy-covered pumps. A 30 mm section was marked in the center of each serpentine segment as a point to measure the time at which the front advanced through these sections. Finally, a round-shape PMMA piece (4 mm high and internal diameter) was connected to the inlet using PSA (Fig. 1C).

2.3 Front position and speed measurements

Vacuum-packed micropumps were opened and attached to the outlet of the microfluidic cartridge. A rectangular-shaped PSA (146-μm thick ARcare 90880, Adhesive Research, Ireland) was employed to assemble the micropumps to the microfluidic devices. These adhesives have been the subject of extensive study in the microfluidic field over the years[25] and have proven to be a useful material for microfluidic bonding in experiments achieving pressures of up to 1000 mbar.[26] After waiting 3 min, the samples (water-based solution of red food-dye) were loaded into the inlet of the device. The advance of the fluid front was recorded on video (OnePlus 6T rear cameras: 16 + 20 megapixels) and from the video images the position, $X(t)$, was extracted.

3 Results and discussion

3.1 Characterization of non-coated PDMS micropumps

3.1.1 Effect of the degassing time (t_d) on non-coated micropumps. First, we evaluated the effect of the degassing time (t_d) of non-coated PDMS micropumps on fluid front dynamics. The system consisted of a multilayer plastic cartridge (0.127 × 1 × 900 mm serpentine) connected to a non-coated PDMS micropump type S (Fig. 1A) after being degassed for 1, 3, 5, 15, 30, 60, 120, or 180 min.

In all cases, during the first 30 min of the experiment (1800 s), the front advanced rapidly with a maximum initial velocity that gradually decreased until the fluid stopped. The maximum initial front velocity increased with the degassing time (t_d), ranging from 0.31 mm s^{-1} for t_d of 1 min to 0.75 mm s^{-1} for t_d of 180 min. Due to the exponential nature of the filling process, the pump's efficiency decreases significantly after a certain point. To define a practical operational limit, we therefore considered the time it takes to reach 80% of the theoretical maximum filling length, X_0. We denote this time as t_{80}, as it represents the point before the filling rate becomes impractically slow. We have chosen this percentage because during this time, rapid pump performance is guaranteed, whereas afterwards, the advance speed of the front is greatly reduced, taking much longer to advance.

This experimental data was fitted to eqn (1) previously reported by Benavent-ClarÒ *et al.*[24]

$$X(t) = X_0\left(1 - e^{-\frac{t}{\tau}}\right). \quad (1)$$

where X is the front flow position through time, X_0 is the position where the front flow stopped and X_0 is a characteristic time related to the time it took to reach the plateau area of the curve. As derived from equation (1), t_{80} is defined as $t_{80} = -\tau \ln(0.2) \approx 1.61\tau$.

Benavent-ClarÒ *et al.*[24] showed that the X_0 value is a terminal distance determined by the channel dimensions, the effective surface of the pump and the degassing time. In the case of uncoated pumps we must take into account the losses due to external surfaces.

Additionally, after obtaining the X_0 value, the characteristic parameter τ was extracted from eqn (1) (Table 1) for the t_d of 15, 60, 120, and 180 min. It was observed that the τ value for pump S tended to increase with longer degassing times, ranging from 21 min (1298 s) for a pump degassed for 15 min to 26 min (1581 s) for a pump degassed for 180 min.

These results indicated that the degassing time (t_d) directly affects the volume of air evacuated from the pump, consequently extending the recovery time required for the pump to restore equilibrium, which is represented by the parameter τ. This correlation is evident in the higher τ values observed when the micropump undergoes longer degassing periods. The characteristic time τ scales approximately as $\tau \propto (VL)/(AK)$,[27] where V is the pump volume, L the diffusion length, A the gas-exchange area, and K the material permeability. This explains the high τ of epoxy-coated pumps, which results from reduced A and extremely low K of the epoxy barrier.

To further analyze the behavior of the fluid front, we utilized the definition of velocity as the derivative of position from eqn (1). This allowed us to derive the following expression:

$$v(t) = \frac{dX(t)}{dt} = v_0 e^{-\frac{t}{\tau}}. \quad (2)$$

where v is the velocity of the fluid front and $v_0 = X_0/\tau$ is the initial velocity of the front. Finally, to obtain the expression for the flow rate of the fluid eqn (3), we used the definition of flow rate in a constant cross section channel and the definition of front velocity eqn (2):

$$Q(t) = A_{ch}\frac{dX(t)}{dt} = Q_0 e^{-\frac{t}{\tau}}. \quad (3)$$

where Q is the flow rate of the fluid front; A_{ch}, the cross section of the channel where the measurements are made; and $Q_0 = \frac{A_{ch}X_0}{\tau}$ is the initial flow of the front.

Table 1 X_0 and τ value calculated for 15, 60, 120 and 180 min of degassing time of non-coated pump S

t_d (min)	X_0 (mm)	τ (s)
15	565	1298
60	725	1471
120	836	1576
180	895	1581

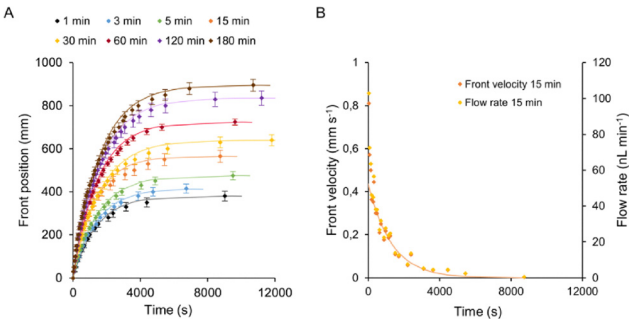

Fig. 2 Effect of td of non-coated micropumps. (A) Plot of the front position of the fluid *versus* time for pump S degassed for various durations, ranging from 1 to 180 min. (B) Plot of the front velocity and the flow rate of the fluid *versus* time produced by a non-coated micropump type S degassed for 15 min. The dots represent the experimental data, while the lines indicate the calculated data using the corresponding eqn (1)–(3). The R^2 values for the fits in (A) are as follows: t_d = 1 min: 0.9906; 3 min: 0.9863; 5 min: 0.9911; 15 min: 0.9857; 30 min: 0.9926; 1 h: 0.9915; 2 h: 0.9955; 3 h: 0.9899.

Fig. 2B shows the calculated flow of the front (lines) and the experimental values obtained for the front velocity and front flow (dots) for a pump type S, degassed during 15 min. The model agrees with the experimental results of front velocity and flow rate of the liquid during the time the pump was actuating. As observed, for pumps subjected to identical degassing times, both the front velocity and fluid flow exhibited a consistent trend throughout the experiment, showcasing an exponential decay as anticipated, indicating the fluid to moves slower as it advances through the channel. However, we observed that the overall front velocity and flow rate increased with the degassing time. For instance, using a 15 min degassed S micropump, the velocity of the front and the fluid flow rate after 12 min of activity were 0.25 mm s^{-1} and 31 nL s^{-1}, respectively. In contrast, the same micropump degassed during 60 min resulted in a front velocity of 0.30 mm s^{-1} and a flow rate of 38 nL s^{-1} after 12 min of activity.

3.1.2 Effect of the effective surface area (S_e) of non-coated micropumps. The effective surface area (S_e) is the specific area of the micropump that is in direct contact with the microchannel, responsible for generating the driving force to move the fluid within the system. In the context of PDMS micropumps, is crucial as it determines the extent of air intake and gas permeation. To evaluate the effect of the effective surface area of non-coated micropumps, three pumps of similar volume and different S_e were used [S (S_e = 683 mm^2), S1 (S_e = 290 mm^2) and S2 (S_e = 92 mm^2)] (Fig. 1A). The micropumps were degassed during 60 and 180 min and then connected to the outlet of the plastic cartridge to trigger fluid movement inside the microchannel (Fig. 1C). It was observed that, for a fixed t_d, a decrease in S_e (S > S1 > S2) resulted in a smaller X_0 value and a lower fluid front velocity leading to an increase in the actuation time (Fig. 3) Based on these results, it is evident that decreasing S_e reduces gas permeation in PDMS micropumps, affecting the exchange of gas molecules during the degassing or the absorption processes. Therefore, with a fixed t_d, the final position and velocity of the fluid front in the microfluidic channel decrease as S_e decreases. Subsequently, τ values were extracted from the model and the effects of t_d and S_e on X_0 and τ were compared (Table 2). For a pump type S, a 200% increase in t_d (from 60 to 180 min) resulted in a 9% increase in τ value. In contrast, a 135% increase in S_e (from S1 to S) led to a 98% decrease in τ value. This indicates that varying S_e had a more significant impact on τ than altering degassing conditions (t_d). Conversely, a 200% increase in t_d for pump S resulted in a 23% increase in the X_0 value. Similarly, a 135% increase in S_e (from S1 to S) led to a 11% increase in the X_0 value. This suggests that the effects of different S_e and t_d values have a comparable impact on X_0.

In summary, variations in S_e and t_d affect τ and X_0 differently.

Table 2 Experimental X_0, experimental ta and calculated τ value for non-coated pumps S, S1 and S2 after 60 or 180 min of degassing

Pump	S_e (mm^2)	t_d (min)	X_0 (mm)	τ (s)	t_{80} (min)
S	683	60	725	1439	39
S1	290	60	645	2854	77
S2	92	60	440	3605	97
S	683	180	895	1574	42
S1	290	180	845	2667	72
S2	92	180	570	3781	101

3.2 Characterization of epoxy-coated PDMS micropumps

3.2.1 Effect of degassing time (t_d) of epoxy-coated micropumps. First, we evaluated the effect of the degassing time of the epoxy-coated micropumps. Neither the volume nor the

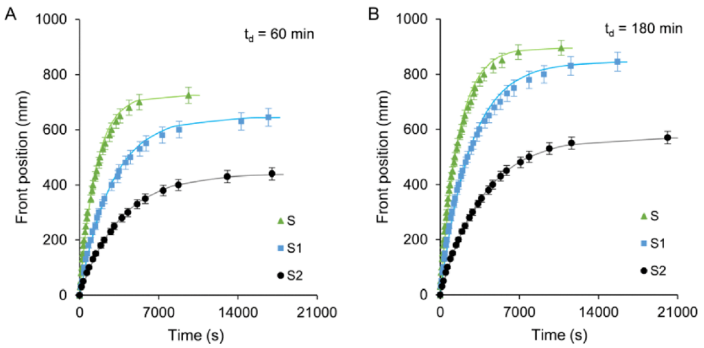

Fig. 3 Effect of the S_e of non-coated micropump. Plot of the fluid front position *versus* time using pumps S, S1 or S2 degassed for 60 min (A) or for 180 min (B). Experimental data points are represented by dots, while lines depict the calculated data using eqn (1). R^2 values for (A): S: 0.9911; S1: 0.9957; S2: 0.9980. For (B): S: 0.9899; S1: 0.9932; S2: 0.9991.

surface area of the PDMS pump are affected during the degassing or reabsorption process. Therefore, the dramatic increase in τ is primarily attributed to the restriction of air recovery pathways due to reduced gas permeability, with no evidence suggesting a significant alteration of the pump's mechanical deformation or stiffness. This interpretation is consistent with the device geometry, scaling arguments, and literature values. The system consisted of a multilayer plastic cartridge (0.127 × 1 × 1800 mm serpentine) connected to an epoxy-coated pump type S, EXP-S (S_e = 683 mm^2), that was degassed during 5, 15 and 30 min. The epoxy-coated pumps exhibited behavior similar to that of the non-coated pumps; the liquid front advanced through the channel with a gradually decreasing velocity until stop. The values of X_0, velocity and actuation times were consistently higher than those obtained with the non-coated micropumps. The dramatic extension of actuation time in epoxy-coated pumps is a direct consequence of the vastly reduced gas permeability of the epoxy resin compared to PDMS. Literature values clearly establish this contrast: PDMS has an extremely high O_2 permeability of approximately (4.5–6) × 10^{-15} m^2 (Pa s)$^{-1}$,[28] whereas typical Araldite epoxies exhibit O_2 permeabilities on the order of (1.1–5.6) × 10^{-18} m^2 (Pa s)$^{-1}$,[29] a reduction of 3 orders of magnitude. Considering the substantial 1 mm thickness of our uniform epoxy layer, and assuming that gas exchange occurs predominantly through the effective surface area S_e, we estimate the overall gas permeability into the coated pumps to be 300–1500 times lower than in their uncoated counterparts. This order-of-magnitude reduction aligns with the observed extension in operational duration. This calculated reduction aligns perfectly with the observed order-of-magnitude increase in operational duration. As an example, when the pump was degassed for 30 minutes, values of X_0 increased from 700 mm to 1810 mm with increasing values of t_d and actuation times. In addition, the channel was filled up to 80% in 36 660 seconds (more than 10 hours), showing the notable increase in the actuation time when the pump is epoxy-coated. (Fig. 4). To the best of our knowledge, an actuation time exceeding 10 hours represents a substantial extension over the typical time operation of degas-driven, PDMS-based self-powered microfluidic systems, which typically operate for up to 1–2 hours. Throughout all

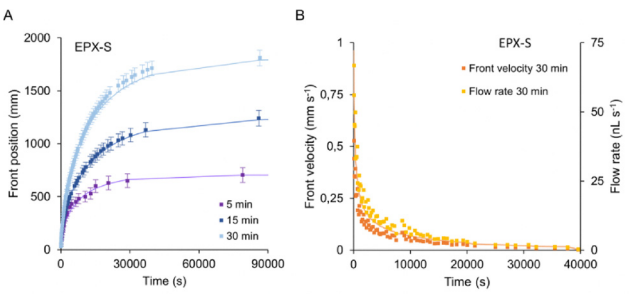

Fig. 4 Effect of t_d of epoxy-coated micropumps on fluid front dynamics. (A) Plot of the front position of the sample *versus* time for pump EPX-S degassed during 5, 15 and 30 min. (B) Plot of the front velocity of the sample *versus* time produced by an epoxy-coated micropump degassed for 30 min. The dots show the experimental data, and the lines show the calculated data using eqn (4)–(6). R^2 values for (A): 5 min: 0.9772; 15 min: 0.9951; 30 min: 0.9885.

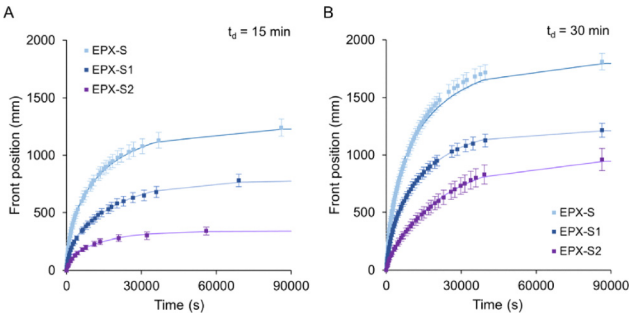

Fig. 5 Effect of Se surface area of the epoxy-coated micropumps. Plot of the fluid front position *versus* time using pumps EPX-S, EPX-S1 or EPX-S2 degassed during the 15 min (A) or 30 min (B). The dots show the experimental data, and the lines show the calculated data using eqn (4). R^2 values for (A) EPX-S: 0.9951; EPX-S1: 0.9925; EPX-S2: 0.9778. For (B) EPX-S: 0.9885; EPX-S1: 0.9942; EPX-S2: 0.9983.

experiments, the epoxy coating demonstrated robust adhesion to the PDMS without any observed cracking, delamination, or blistering. Furthermore, pumps subjected to multiple degassing–actuation cycles during system optimization showed no significant degradation in performance parameters (X_0 or τ) or signs of air leakage, indicating promising reusability and stability.

3.2.2 Effect of the effective surface area (S_e) of the epoxy-coated micropumps. To evaluate the effect of S_e of the epoxy-coated micropumps, three non-coated pumps of similar volume but different S_e were used: EPX-S (S_e = 683 mm^2), EPX-S1 (S_e = 290 mm^2), and EPX-S2 (S_e = 92 mm^2) (Fig. 1B). The micropumps were degassed for 15 or 30 min and then connected to the outlet of the plastic cartridge. The behavior observed was similar to that of the non-coated micropumps: for a fixed t_d, a decrease in S_e resulted in a smaller X_0 value and a lower fluid front velocity, leading to an increase in the actuation time of the pump (Fig. 5).

3.3 Comparison of non-coated and epoxy-coated micropumps

We observed a significant difference in performance between coated and non-coated micropumps, which is due to their respective abilities to recover air after degassing. Due to their design, non-coated pumps rapidly become saturated with air because all six sides are exposed, allowing air to permeate from every direction. In contrast, epoxy-coated pumps are designed to prevent such leakage; only the effective surface area (S_e), which is in contact with the microchannel, is exposed to air, generating the driving force to move the fluid. This configuration limits air intake to just the S_e, leading to a slower air recovery rate in epoxy-coated pumps compared to the faster recovery rate in non-coated pumps, where all six sides facilitate air intake. These differences in air recovery capabilities could account for the distinct performance characteristics observed between non-coated and coated pumps. To evaluate the effect of the characteristic air recovery time of the pumps, which is the time required for the pump to reach equilibrium after vacuum, non-coated micropumps (S, S1, and S2) and epoxy-coated micropumps (EPX-S, EPX-S1, and EPX-S2) were degassed for 15 or 30 minutes and then connected to the outlet of a 1800 mm long serpentine channel (Fig. 1C). The experiment

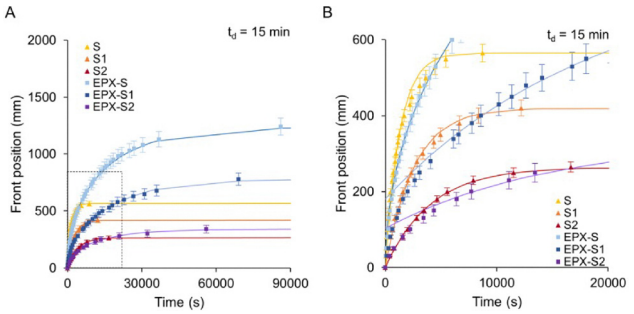

Fig. 6 Effect of the recovery rate of the micropump on fluid front dynamics. Plot (A) and magnification of the first 30 min (B) of the front position of the fluid *versus* time, driven by pumps S, S1, S2, EPX-S, EPX-S1 and EPX-S2 degassed during 15 min. The dots show the experimental data, and the lines show the calculated data using the eqn (1) and (4) for non-coated and epoxy-coated respectively. R^2 values: S: 0.9857; S1: 0.9774; S2: 0.9370; EPX-S: 0.9951; EPX-S1: 0.9925; EPX-S2: 0.9778.

showed a similar general trend for both types of pumps, but the non-coated pumps reached equilibrium more quickly than the epoxy-coated pumps, which achieved a higher X_0 value. Specifically, the epoxy coating of pump S resulted in a 180% increase in X_0 value compared to the non-coated pump (for a t_d of 30 min). Additionally, the actuation time of the pumps, and consequently the τ values, were significantly higher for epoxy-coated pumps, achieving nearly ten times longer operating time in epoxy-coated pumps (Fig. 6).

While the experimental data for the non-coated pumps was fitted to eqn (1), velocity and the flow could be calculated with eqn (2) and (3), the data of the epoxy-coated pumps could only be fitted with eqn (1) during the first minutes of the experiment (short-term times). On the other hand, the experimental results obtained with the epoxy-coated micropumps could be fitted using a new equation, which was mathematically derived in ref. 24:

$$X(t) = X_0\left(1 - e^{-\frac{t}{\tau}}\right)^{\frac{1}{2}}. \quad (4)$$

In eqn (4) the scaling behavior is governed by a power law of 1/2. Experimentally, we found that all epoxy-coated pumps obey this expression.

In addition, to obtain the expression for the front flow, we derived the front position model eqn (4) to obtain the front velocity:

$$v(t) = \frac{dX(t)}{dt} = v_0 \frac{e^{-\frac{t}{\tau}}}{\left(1 - e^{-\frac{t}{\tau}}\right)^{\frac{1}{2}}}. \quad (5)$$

where v is the velocity of the fluid front and, in this case, $v_0 = X_0/2\tau$ is a characteristic velocity. Then we multiplied it for the cross section of the channel to obtain the front flow:

$$Q(t) = A_{ch}\frac{dX(t)}{dt} = Q_0 \frac{e^{-\frac{t}{\tau}}}{\left(1 - e^{-\frac{t}{\tau}}\right)^{\frac{1}{2}}}. \quad (6)$$

where Q is the flow rate of the fluid front; A_{ch}, the cross section of the channel where the measurements are made; and $Q_0 = \frac{A_{ch}X_0}{\tau}$ is the initial flow of the front.

Table 3 Experimental X_0 and calculated τ for non-coated pumps S, S1, S2, and epoxy-coated pumps, EPX-S, EPX-S1 and EPX-S2 after 15 or 30 min of degassing

Pump	Degas. time (min)	X_0 value (mm)	τ value (s)
S	15	565	1298
S1	15	420	2585
S2	15	265	4067
EPX-S	15	1240	22 172
EPX-S1	15	780	27 280
EPX-S2	15	340	20 424
S	30	640	1594
S1	30	540	2753
S2	30	340	3658
EPX-S	30	1810	22 770
EPX-S1	30	1215	24 695
EPX-S2	30	960	35 000

Once the mathematical models were validated for non-coated and epoxy-coated pumps, we performed a quantitative comparison of air recovery rates or pump performance by calculating the τ value corresponding to the different micropumps using eqn (1) for the non-coated and eqn (4) for the epoxy-coated pumps. The τ values of the epoxy-coated pumps were significantly higher than those of the non-coated pumps, ranging from 21 min (1298 s) for non-coated pump type S to over 9 h (more than 35 000 s) for epoxy-coated pump EPX-S2 (Table 3). The model successfully reproduces fluid front dynamics across all tested pump geometries and degassing conditions, with extracted parameters (τ, X_0) showing consistent physical trends. It serves as a predictive framework for this family of degas-driven devices, providing a powerful tool for designing customized pumps within the characterized operational space, though broader validation would be needed for extended conditions.

These results indicate that to design pumps with very long actuation times, epoxy-coated pumps should be used. The flow rate will largely depend on the effective surface area (S_e); the greater S_e, the greater the flow velocity. Moreover, the amount of air that can be displaced is influenced by the degassing time, where longer degassing allows for greater air displacement. Taking these design rules into account new customized autonomous micropumps can be designed for different applications. The theoretical maximum actuation time is achieved by maximizing the volume of air removed during degassing and minimizing the pump's overall gas permeability. However, these two factors are linked to a critical trade-off: reducing the permeability of the gas-exchange surface (S_e) also reduces the initial flow rate (Q_0). Our design strategy of coating only the external surfaces optimally balances this trade-off. It drastically increases the actuation time by restricting air intake pathways, without compromising the flow rate generated by the high-permeability PDMS at the effective surface.

4 Conclusions

This study reports a significant advance in self-powered microfluidics: epoxy-coated PDMS micropumps capable of sustained operation for over 10 hours. This represents a ten-fold increase in operational duration compared to traditional, non-coated pumps. By characterizing modular polymeric micropumps across their full range of actuation, we show their potential

for providing self-powered flow control over intermediate durations, ranging from an hour to nearly half a day. Using these calibration curves, we compared mathematical models to predict flow rates, actuation times, and the τ value, which is crucial to indicate the air recovery rate and therefore the actuation time of the micropumps. These models facilitate the design of customized self-powered microsystems for both short-term and long-term applications. Our investigation underscores the significant impact of degassing time, effective surface area, and air recovery rate on the fluid dynamics within the microchannel.

The flow rates generated by our pumps, while low and decaying, are suitable for numerous microfluidic applications. In biological contexts, such as organ-on-chip and prolonged cell culture, these gentle, nL s^{-1} flow rates are often required to maintain low-shear environments and preserve vital biochemical gradients. For analytical applications, including passive sampling and assays requiring long incubation times, the sustained, autonomous operation over 10 hours is a key advantage over faster, short-lived pumping strategies. Thus, the operational profile of these epoxy-coated pumps, which are self-powered, low-flow, and long-lasting, makes them well-suited for portable diagnostic and monitoring systems where simplicity and extended runtime are paramount.

This work builds on our previous reports on the description of a universal modular microfluidic architecture for self-powered microfluidics[19,20] where we showed that these systems are suitable for different fluidics operations. Microfluidics cartridges and micropumps may be fabricated on different materials and several fast prototyping and manufacturing techniques including 3D printing.

We believe this advancement, specifically the ability to easily tune pump performance for long-term operation, will contribute to the performance and applicability of autonomous microfluidic systems across biomedical diagnostics, environmental monitoring, and industrial processes, paving the way for future innovations in portable and efficient microfluidic technologies.

Conflicts of interest

There are no conflicts to declare.

Data availability

The experimental datasets (raw video files, flow tracking data, and fitting parameters) generated during this study are not deposited in a public repository due to their large size and specialized format but are available from the corresponding author, Lourdes Basabe-Desmonts, upon reasonable request.

Acknowledgements

YA-B, FB-L and LB-D acknowledge funding support from the Ministerio de Ciencia, Innovaciòn y Universidades, the Agencia Estatal de Investigaciòn (AEI, 10.13039/501100011033), and the European Regional Development Fund (FEDER, EU), under project PID2024-155781NB-I00. and from Basque Government under "Grupos Consolidados" with Grant No. IT1633-22. AB-C and AH-M acknowledge support from "Ministerio de Ciencia, Innovaciòn y Universidades" (Spain) under project PID2022-137994NB-I00 and AGAUR (Generalitat de Catalunya) under project 2021-SGR-00450. We all acknowledge the support of the Spanish Ministry of Economy and Competitiveness through grant DPI2015-71901-REDT (MIFLUNET), partly funded through European Funds.

Notes and references

1 V. Iyer, Z. Yang, J. Ko, R. Weissleder and D. Issadore, *Lab Chip*, 2022, **22**, 3110–3121.
2 S. F. Berlanda, M. Breitfeld, C. L. Dietsche and P. S. Dittrich, *Anal. Chem.*, 2020, **93**, 311–331.
3 D. Vloemans, L. Van Hileghem, H. Ordutowski, F. Dal Dosso, D. Spasic and J. Lammertyn, *Microfluidics Diagnostics: Methods and Protocols*, Springer, 2024, pp. 3–50.
4 J. Park and J.-K. Park, *Lab Chip*, 2019, **19**, 2973–2977.
5 C. Srisomwat, P. Teengam, N. Chuaypen, P. Tangkijvanich, T. Vilaivan and O. Chailapakul, *Sens. Actuators, B*, 2020, **316**, 128077.
6 M. T. Guler, Z. Isiksacan, M. Serhatlioglu and C. Elbuken, *Sens. Actuators, B*, 2018, **273**, 350–357.
7 J. Ko, D. Park, J. Lee, S. Jung, K. Baek, K. E. Sung, J. Lee and N. L. Jeon, *Nat. Rev. Bioeng.*, 2024, **2**, 453–469.
8 S. M. Grist, S. S. Nasseri, L. Laplatine, J. C. Schmok, D. Yao, J. Hua, L. Chrostowski and K. C. Cheung, *Sci. Rep.*, 2019, **9**, 17782.
9 A. A. Folgueiras-Amador, K. Philipps, S. Guilbaud, J. Poelakker and T. Wirth, *Angew. Chem., Int. Ed.*, 2017, **56**, 15446–15450.
10 S. Mashaghi, A. Abbaspourrad, D. A. Weitz and A. M. van Oijen, *TrAC, Trends Anal. Chem.*, 2016, **82**, 118–125.
11 M. Ripoll, E. Martin, M. Enot, O. Robbe, C. Rapisarda, M.-C. Nicolai, A. Deliot, P. Tabeling, J.-R. Authelin and M. Nakach, *et al.*, *Sci. Rep.*, 2022, **12**, 9483.
12 M. Eichler, C.-P. Klages and K. Lachmann, *Microsystems for Pharmatechnology: Manipulation of Fluids, Particles, Droplets, and Cells*, Springer, 2016, pp. 59–97.
13 M. Uh, J.-S. Kim, J.-H. Park, D. H. Jeong, H.-Y. Lee, S.-M. Lee and S.-K. Lee, *J. Nanosci. Nanotechnol.*, 2017, **17**, 1083–1091.
14 L. Xu, A. Wang, X. Li and K. W. Oh, *Biomicrofluidics*, 2020, **14**, 031503.
15 K. Hosokawa, K. Sato, N. Ichikawa and M. Maeda, *Lab Chip*, 2004, **4**, 181–185.
16 K. Hosokawa, M. Omata and M. Maeda, *Anal. Chem.*, 2007, **79**, 6000–6004.
17 I. K. Dimov, L. Basabe-Desmonts, J. L. Garcia-Cordero, B. M. Ross, A. J. Ricco and L. P. Lee, *Lab Chip*, 2011, **11**, 845–850.
18 S. Izaddoust, I. Poves-Ruiz, E. A. Hualde, D. Patko, L. Florea, C. Delaney, L. Basabe-Desmonts and F. Benito-Lopez, *Lab Chip*, 2025, **25**, 6075–6099.
19 J. Etxebarria-Elezgarai, Y. Alvarez-Braña, R. Garoz-Sanchez, F. Benito-Lopez and L. Basabe-Desmonts, *Ind. Eng. Chem. Res.*, 2020, **59**, 22485–22491.
20 Y. Alvarez-Braña, J. Etxebarria-Elezgarai, L. R. de Larrinaga-Vicente, F. Benito-Lopez and L. Basabe-Desmonts, *Sens. Actuators, B*, 2021, **342**, 129991.

21 G. Li, Y. Luo, Q. Chen, L. Liao and J. Zhao, *Biomicrofluidics*, 2012, **6**(1), 014118.
22 P. Tabeling, *Introduction to microfluidics*, Oxford university press, 2023.
23 F. Del Giudice, *Micromachines*, 2022, **13**, 167.
24 A. Benavent-Claró, Y. Alvarez-Braña, F. Benito-Lopez, L. Basabe-Desmonts and A. Hernandez-Machado, *Phys. Fluids*, 2025, **37**, 027202.
25 K. Giri and C.-W. Tsao, *Micromachines*, 2022, **13**, 486.
26 J. Saez, L. Basabe-Desmonts and F. Benito-Lopez, *Microfluid. Nanofluid.*, 2016, **20**, 116.
27 S. O. Woo, M. Oh, K. Nietfeld, B. Boehler and Y. Choi, *Biomicrofluidics*, 2021, **15**, 034106.
28 T. Merkel, V. Bondar, K. Nagai, B. Freeman and I. Pinnau, *J. Polym. Sci., Part B: Polym. Phys.*, 2000, **38**, 415–434.
29 M. C. Celina and A. Quintana, *Polymer*, 2018, **150**, 326–342.

